Available online at www.sciencedirect.com
SCIENCE DIRECT
Journal of Molecular Structure 788 (2006) 22–29
Journal of MOLECULAR STRUCTURE
www.elsevier.com/locate/molstruc

X-ray crystallographic and 2D HETCOR NMR studies of 2-acetylthiophene-*o*-aminobenzoylhydrazone: synthesis and spectral studies of its transition metal complexes

Kalagouda B. Gudasi [a,*], Rashmi V. Shenoy [a], Ramesh S. Vadavi [a], Siddappa A. Patil [a], Munirathinam Nethaji [b]

[a] *Department of Chemistry, Karnatak University, Dharwad -580 003, Karnataka, India*
[b] *Inorganic and Physical Chemistry, Indian Institute of Science, Bangalore-560 012, India*

Received 12 August 2005; received in revised form 7 November 2005; accepted 10 November 2005
Available online 14 February 2006

Abstract

The coordination chemistry of the ligand 2-acetylthiophene-*o*-aminobenzoylhydrazone (ATABZ) with oxovanadium(IV), manganese(II), cobalt(II), nickel(II), copper(II), zinc(II) and cadmium(II) has been studied wherein the complexes were characterized by elemental analyses, magnetic moments, conductivity measurements, spectral (IR, 1D and 2D HETCOR NMR, EPR and UV-VIS) and thermal studies. The ligand ATABZ crystallizes in the orthorhombic system, space group *Pca21* with lattice parameters $a=8.5279(17)$ Å, $b=5.8101(11)$ Å, $c=25.720(5)$ Å, $V=1274.3(4)$ Å^3 and $Z=4$. All the complexes are neutral in nature and possess four-coordinate geometry around the metal ion except oxovanadium(IV) complex, which is five-coordinate. The X-band EPR spectra of the copper(II) and oxovanadium(IV) complexes at both room temperature and liquid nitrogen temperature have been recorded and their salient features are reported. The antibacterial and antifungal activities of the ligand and complexes have been carried out.

Keywords: 2-Acetylthiophene; Hydrazone ligand; Transition metal complexes; X-ray structure determination

1. Introduction

Hydrazones are a versatile class of ligands having great physiological and biological activities, and have found use as insecticides, anticoagulants, antitumour agents, antioxidants and plant growth regulators [1]. Their metal complexes have found applications in various chemical processes like nonlinear optics, sensors, medicine, etc. [2]. Furthermore, hydrazones incorporating heterocyclic moieties are well known for their metal binding ability and exhibit interesting coordinating behavior with transition metal ions [3,4], which makes them interesting from the structural point of view also.

Of the heterocyclic moieties the thiophene ring system is ubiquitous in nature and is known to exhibit antifungal, bacteriostatic, analgesic and anti-inflammatory activities [5]. Especially, the 2-substituted thiophenes are an important constituent of the drugs methapyrilene, temidap, tienilic acid and temocillin [6]. The metal complexes of thiosemicarbazones containing the thiophene moiety have exhibited enhanced antiamoebic activity [7].

Knowledge of the structural peculiarities of a biologically active molecule and its inherent 3 -dimensional structure is a necessary condition for investigating the interaction with metal ions and for designing new compounds. To gain an insight into the conformational aspects of the title ligand and in order to study its coordination behavior towards transition metal ions, we have designed and synthesized a compound by condensing two biologically active moieties, *o*-aminobenzoylhydrazide [8] with 2-acetylthiophene.

The single crystal structures of a few hydrazones derived from *o*-aminobenzoylhydrazide have been reported [9–11]. In the present work, we report for the first time, the X-ray crystal structure of 2-acetylthiophene-*o*-aminobenzoylhydrazone (ATABZ) and the synthesis, characterization and biological evaluation of its oxovanadium(IV), manganese(II), cobalt(II), copper(II), nickel(II), zinc(II) and cadmium(II) complexes.

* Corresponding author. Tel.: +91 836 2460129/215286; fax: +91 836 2771275.
E-mail address: kbgudasi@rediffmail.com (K.B. Gudasi).

0022-2860/$ - see front matter © 2006 Elsevier B.V. All rights reserved.
doi:10.1016/j.molstruc.2005.11.012

Table 1
Analytical and physicochemical data of ATABZ and its transition metal complexes

Compound	Elemental analyses(%)[a]						Electronic spectral data[b] (cm^{-1})	μ_{eff}	Λ_M[c]
	M	C	H	N	Cl	SO_4			
ATABZ	–	60.0 (60.15)	5.05 (5.0)	15.99 (16.10)	–	–	30,769; 28,169	Dia	–
(Mn(ATABZ)Cl_2)	14.20 (14.27)	40.47 (40.54)	3.36 (3.37)	10.05 (10.90)	18.40 (18.42)	–	25,706; 27,397; 29,154	5.73	0.49
(Co(ATABZ)Cl_2)	15.10 (15.15)	40.0 (40.12)	3.15 (3.34)	10.78 (10.80)	18.15 (18.23)	–	15,243; 16,583; 25,585	4.46	0.47
(Ni(ATABZ)Cl_2)	15.0 (15.10)	40.15 (40.14)	3.30 (3.34)	10.77 (10.80)	18.20 (18.24)	–	14,598; 25,641	3.45	0.56
(Cu(ATABZ)Cl_2)	16.10 (16.15)	39.63 (39.65)	3.29 (3.30)	10.62 (10.67)	18.05 (18.02)	–	14,285–13,157; 23,752	1.74	0.41
(Zn(ATABZ)Cl_2)	16.50 (16.54)	39.42 (39.46)	3.25 (3.28)	10.61 (10.62)	17.91 (17.93)	–	28,571	Dia	0.42
(Cd(ATABZ)Cl_2)	25.38 (25.41)	35.22 (35.27)	2.90 (2.93)	9.41 (9.49)	16.0 (16.03)	–	27,397	Dia	0.51
(VO(ATABZ) SO_4 H_2O)	11.51 (11.57)	35.40 (35.45)	3.35 (3.40)	9.49 (9.54)	–	21.79 (21.86)	11,100; 16,638	1.72	0.48

[a] Calculated values are in parentheses.
[b] In DMSO.
[c] $Ohm^{-1}\ cm^2\ mol^{-1}$; Dia = diamagnetic.

2. Experimental

2.1. Materials and general methods

All chemicals were of A.R. grade and were used without further purification. Methyl anthranilate (S.D. Fine-chem), hydrazine hydrate (Rankem) and 2-acetylthiophene (Sisco-Chem) were used as obtained. *o*-Aminobenzoylhydrazide was prepared by an earlier method [12].

Elemental analyses of the ligand and complexes were performed on a thermoquest CHN analyzer. The complexes were analyzed for their metal content by EDTA titration after decomposition with a mixture of HCl and $HClO_4$. The chloride content was determined as AgCl after decomposition with HNO_3. The sulphate content in the VO(IV) complex was determined as barium sulphate, gravimetrically. The IR spectra were recorded as KBr pellets in the 4000–400 cm^{-1} region on a Nicolet 170 SX FT-IR spectrometer. Electronic absorption spectra were measured in DMSO with a Cary-Bio 50 Varian spectrophotometer. The 1D and 2D NMR spectra of the ligand were recorded in dmso-d_6 on a Bruker AMX 500 spectrometer operating at 500.13 MHz for ^1H and 127.77 for ^{13}C using a 5 mm $^1H/^{13}C$ dual probe. The ^1H and ^{13}C NMR spectra of the cadmium(II) complex were recorded on a Bruker Avance 300 spectrometer operating at 300.13 MHz for ^1H and 75.47 MHz for ^{13}C using a 5 mm $^1H/^{13}C$ dual probe. Magnetic susceptibility measurements were made at room temperature on a Faraday balance using $Hg[Co(CNS)_4]$ as the calibrant and the diamagnetic corrections were made by direct weighing of the ligand for diamagnetic pull. Conductance measurements were recorded in DMSO (10^{-3} M) using an ELICO-CM-82 conductivity bridge with platinum electrodes and cell constant 0.53. Thermogravimetric analyses of the complexes were carried out under N_2 atmosphere in the 25–1000 °C range at a heating rate of 10 °C/min using a TGA Analyzer, Perkin Elmer, US. EPR spectra of the copper(II) and oxovanadium(IV) complexes were recorded with a Varian E4 X-band spectrometer at both RT and LNT using TCNE as 'g' marker.

2.2. Syntheses

2.2.1. 2-Acetylthiophene-o-aminobenzoylhydrazone (ATABZ) (Scheme 1)

2-Acetylthiophene (10.8 g, 100 mmol) was added to a methanolic (130 cm^3) solution of *o*-aminobenzoylhydrazone (15.1 g, 100 mmol) and the mixture was stirred for 2–3 h to yield a yellow crystalline product. Completion of the reaction was checked by TLC on precoated silica gel plates. The isolated compound was filtered as yellow crystals, washed with cold ethanol and dried in air. Recrystallization from hot methanol yielded the light yellow crystals of ATABZ. m.p. 198–200 °C, yield: 87%.

2.2.2. Preparation of complexes

To a clear hot solution of ATABZ (0.259 g, 1 mmol) in 25 cm^3 methanol was added 1 mmol of metal chloride/sulphate

and stirred for 3–4 h. The solution was then concentrated to a small volume and the precipitate obtained was filtered, washed with cold ethanol and air-dried. Attempts to grow single crystals of the complexes were unsuccessful. Yield: 69–74%.

2.3. X-ray crystallography

The crystal structure of the title compound was determined by single crystal X-ray diffraction with dimensions of $0.62\times 0.51\times 0.33\ mm^3$. The data were collected on a BRUKER SMART APEX CCD Diffractometer at 293 K, using graphite-monochromatized MoKα radiation ($\lambda=0.71073$ Å) and scan mode in the range 3.17–28.02. The structure was solved by direct methods and refined by Full-matrix least squares on F^2. All of the non-hydrogen atoms were refined with anisotropic temperature factors. The calculations were performed using the SHELXTL programme [13]. Crystallographic data of ATABZ have been deposited at the Cambridge Crystallographic Data Centre (CCDC), 12 Union Road, Cambridge CBZ 1EZ, UK. Copies of the data can be obtained free of charge by quoting the deposition number 269110.

3. Results and discussion

The elemental analyses, magnetic moments and conductivity data are presented in Table 1. All the metal complexes possess 1:1 (M: L) stoichiometry. The complexes are soluble in EtOH, MeOH, $CHCl_3$, DMF and DMSO but are insoluble in CCl_4, C_6H_6 and H_2O. The molar conductance values of the complexes ranging from 0.41–0.56 $Ohm^{-1}\,cm^2\,mol^{-1}$ reveal their non-electrolytic nature [14].

3.1. Description and discussion of the crystal structure of ATABZ

The crystal data, structure refinement and selected bond lengths and bond angles of ATABZ are given in Tables 2 and 3, respectively. The ORTEP [15] and molecular packing diagrams are depicted in Figs. 1 and 2 respectively. The analysis of the crystal structure of ATABZ evidences that it is coplanar. The average C–C bond lengths and bond angles of the phenyl ring (Fig. 1) lie between 1.316–1.418 Å and 117–123.09°, respectively, which is similar to the analogous compound di-2-pyridylketone-2-aminobenzoylhydrazone [16]. All the C–C bond lengths [1.364 Å] and C–C–C angles [112.56°] of the thiophene ring as well as the C–S bond lengths [1.70 Å] and C–S–C angle [92.16°] are in accordance with that of a typical thiophene moiety [17]. The C=O [C(6)-O(1)] displays a bond distance of 1.234 Å which is consistent with a carbonyl double bond [18]. The C(7)-C(6)-N(2) angle is 118.7° as for an sp^2 hybridized carbon[(6)]. The ligand lies in two planes with plane I [C(7), C(8), C(9), C(10), C(11), C(12)] making a dihedral angle of 175.55° with plane II [S(1), C(1), C(2),C(3), C(4)]. The conformational designations across C(6)-C(7)-C(8)-N(3) and O(1)-C(6)-C(7)-C(8) indicate the *+synperiplanar* arrangement and the corresponding torsional angles are +5.64 and +17.95°, respectively. The torsional angle of −177.46° exhibited by S(1)-C(4)-C(5)-C(13) indicate the C(13) of the methyl group to be in a *trans* position to the sulphur of the thiophene moiety. The torsional angles S(1)-C(4)-C(5)-N(1) [+2.24 Å] and N(1)-N(2)-C(6)-O(1) [−5.11 Å] indicate that S(1), N(1) and O(1) are *cis* to each other. The molecular packing diagram (Fig. 2) shows

Table 2
Crystal data and structure refinement of ATABZ

Empirical formula	$C_{13}H_{13}N_3OS$
Formula weight	259.32
Temperature, K	293
Crystal system	Orthorhombic
Space group	Pca21
Unit cell dimensions	$a=8.5279(17)$ Å $\alpha=\beta=\gamma=90°$
	$b=5.8101(11)$ Å
	$c=25.720(5)$ Å
V, Å^3	1274.3(4)
Z	4
Density (calculated)(mg/m^3)	1.3516
Habit	Rectangular
Absorption coefficient (mm^{-1})	0.245
λ, Å	0.71073
F(000)	544
Range (°) for data collection	3.17–28.02
No. of reflections measured	9374
No. of unique reflections	2974
R(Int)	0.0332
No. of observed reflections	2342
Refinement method	Full matrix least squares on F^2
Final R indices ($I>2\sigma$ (I))	0.0617
Goodness-of-Fit-on F^2	1.115
Final R indices (all data)	0.0825

Table 3
Selected bond lengths (Å) and angles (°) for ATABZ

Atom	Bond lengths	Atom	Bond lengths
S(1)-C1	1.697(4)	C(4)-C(5)	1.466(4)
S(1)-C4	1.712(3)	C(5)-C(13)	1.485(5)
O(1)-C(6)	1.234(3)	C(6)-C(7)	1.486(4)
N(1)-N(2)	1.384(4)	C(7)-C(8)	1.418(4)
N(1)-C(5)	1.276(4)	C(7)-C(12)	1.388(4)
N(2)-C(6)	1.355(4)	C(8)-C(9)	1.411(5)
N(3)-C(8)	1.350(5)	C(9)-C(10)	1.367(5)
C(1)-C(2)	1.318(7)	C(10)-C(11)	1.385(5)
C(2)-C(3)	1.411(6)	C(11)-C(12)	1.362(5)
C(3)-C(4)	1.365(5)		
Atom	Bond angles	Atom	Bond angles
C(1)-S(1)-C(4)	92.2(2)	C(8)-C(7)-C(6)	119.1(3)
C(5)-N(1)-N(2)	119.0(3)	C(12)-C(7)-C(6)	122.1(3)
C(6)-N(2)-N(1)	116.8(3)	C(12)-C(7)-C(8)	118.6(3)
C(2)-C(1)-S(1)	111.9(4)	N(3)-C(8)-C(7)	123.2(3)
C(1)-C(2)-C(3)	113.6(4)	N(3)-C(8)-C(9)	119.2(3)
C(3)-C(4)-S(1)	110.1(3)	C(9)-C(8)-C(7)	117.5(3)
C(5)-C(4)-S(1)	119.5(2)	C(10)-C(9)-C(8)	121.5(3)
C(3)-C(4)-C(5)	130.4(3)	C(9)-C(10)-C(11)	120.7(3)
C(4)-C(5)-C(13)	119.0(3)	C(9)-C(10)-C(11)	120.7(3)
O(1)-C(6)-N(2)	120.0(3)	C(12)-C(11)-C(10)	118.6(4)
O(1)-C(6)-C(7)	121.2(3)	C(11)-C(12)-C(7)	123.1(3)
N(2)-C(6)-C(7)	118.7(3)		

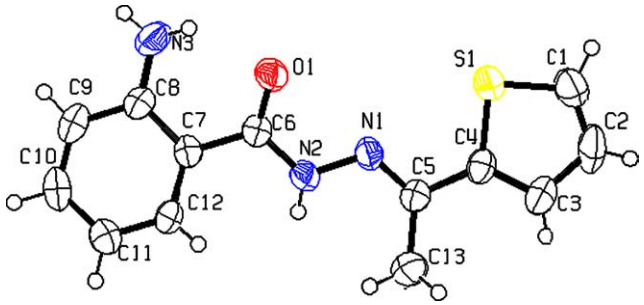

Fig. 1. ORTEP diagram of ATABZ.

the presence of one intra molecular and two intermolecular hydrogen bondings. One of the hydrogens [H3A] of N(3) of NH_2 group is involved in intra molecular hydrogen bonding with the O(1) of the C=O entity. The O(1) of the carbonyl group also acts as an acceptor to H(12) of the phenyl ring and H(2A) of the NH group of another molecule. The N(2A)-H(2A)···O(1)[I] ([I] $=x-1/2, -y, +z$) distance (2.943 Å) is shorter than the C(12)-H(12)··· O(1)[I] distance of 3.225 Å whereas the N(3)-H(3A)··· O(1)[0] ([0]$=x, y, z$) distance is 2.655 Å. Interestingly these hydrogen bonds link the molecules in a helical-like structure as shown in Fig. 3.

3.2. EPR spectra

The EPR spectra of the polycrystalline sample of [Cu(ATABZ)Cl_2] showed identical features at both room temperature (RT) and liquid nitrogen temperature (LNT) with two $g\|$ and one $g\perp$ values. The g values obtained are $g\|_1=2.16$, $g\|_2=2.24$ and $g\perp=2.10$ (at RT) and $g\|_1=2.15$, $g\|_2=2.23$ and $g\perp=2.09$ (at LNT). The $g\| > g\perp >$ ge (2.00277) indicates the localization of the unpaired electron in the $d_{x^2-y^2}$ orbital.

The $g\|$ value is less than 2.3 indicating the covalent nature of the metal-ligand bonding [19]. The axial factor G is 2.5 (RT) and 2.4 (LNT), which is less than 4 indicates considerable metal–metal interaction in the complex [20]. This is also supported by its magnetic moment value, which is slightly decreased.

The EPR spectrum of the polycrystalline oxovanadium(IV) complex (Fig. 4) at room temperature exhibits an eight-line pattern corresponding to the well resolved parallel and perpendicular components of g-and hyperfine (hf) A -tensors. The various spin-Hamiltonian parameters have been calculated and are as follows: $g\|=2.01$, $g\perp=2.02$, $g_0=2.01$, $A\|=-85.71$, $A\perp=10$ and A_0 (isotropic hf parameter) $=-21.90$. The trend $ge<g\|<g\perp$ shows the presence of the unpaired electron in the d_{xy} orbital. Using the values of E1 (16,620 cm^{-1}) and E2 (11,100 cm^{-1}) obtained from electronic absorption spectra and the above g parameters, the spin-orbit coupling constant (λ) has been calculated using the relations,

$$g\| = ge - \frac{8\lambda}{E1} \quad \text{and} \quad g\perp = ge - \frac{2\lambda}{E2}$$

According to Kivelson and Lee [21], a theoretical value of 170 cm^{-1} is predicted for λ for C_{4V} symmetry. In the present case, the λ value obtained is 55 cm^{-1}, the reduction in its value for the double bonded oxovanadium $(V{=}O)^{2+}$ complex being attributed to the substantial π bonding.

3.3. UV spectra

The Uv-visible spectra of ligand and complexes were taken in order to assign the geometries around the metal ions. The electronic spectrum of the ligand APABZ showed two strong bands at 30,769 and 28,169 cm^{-1} assignable to the $n-\pi^*$ transitions.

The electronic spectrum of the manganese(II) complex shows three bands at 25,706, 27,397 and 29,154 cm^{-1} which are assigned to the $^6A_1 \rightarrow {}^4E$, $^6A_1 \rightarrow {}^4T_2$(D) and $^6A_1 \rightarrow {}^4$E(D) transitions, respectively as for a tetrahedrally coordinated manganese(II) ion. The magnetic moment value of 5.73 BM obtained supports this assignment.

The electronic spectrum of the nickel(II) complex shows a single band at 14,598 cm^{-1} assigned to the $^3T_1(E) \rightarrow {}^3T_1(P)$ transition which is consistent with a tetrahedral geometry. The broad band at 25,641 cm^{-1} tailing into the visible region is assigned to the charge-transfer band [3].

In the electronic spectrum of cobalt(II) complex, two bands observed at 15,243 and 25,585 cm^{-1} are due to

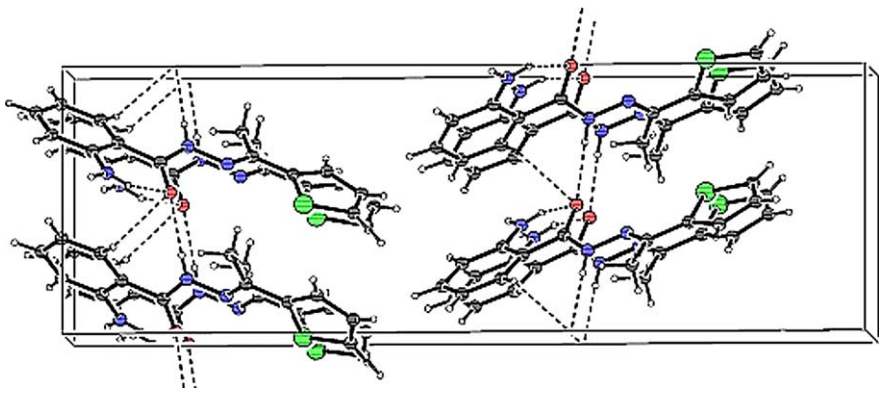

Fig. 2. Molecular packing diagram of ATABZ showing the intra-and intermolecular hydrogen bondings.

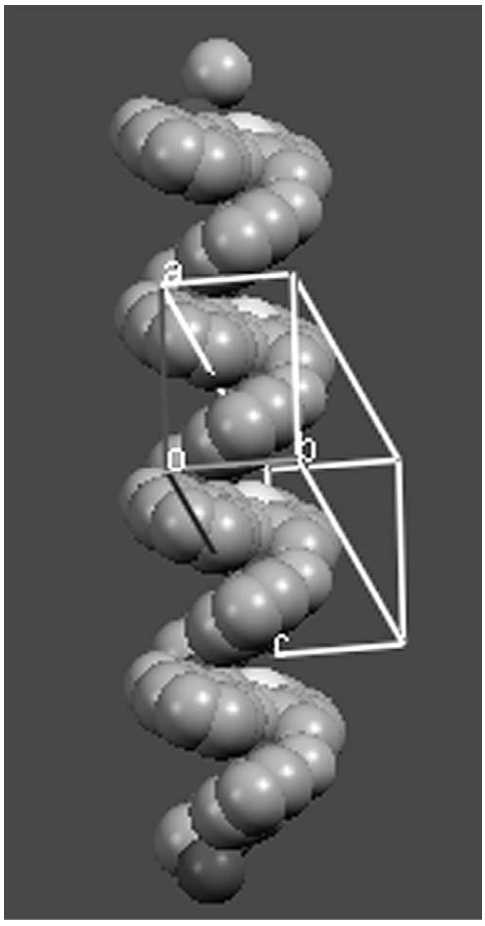

Fig. 3. Helical-like structure of ATABZ shown in space filling mode.

$^4A_2(F) \rightarrow {}^4T_1(P)$ transitions. A weak band at 16,583 cm^{-1} is due to spin–spin coupling. These assignments are supported by the μ_{eff} value of 4.46 BM which is consistent with tetrahedral configuration around the cobalt(II) ion.

The broad band between 14,285–13,157 cm^{-1} in the electronic spectrum of the copper(II) complex is formed by the combination of the $^2B_{1g} \rightarrow {}^2A_{1g}$ and $^2B_{1g} \rightarrow {}^2E_g$ transition as for a square planar configuration around the Cu(II) ion. A broad band centered at 28,571 and 27,397 cm^{-1} in the zinc(II) and cadmium(II) complexes, respectively was assigned to the charge-transfer transitions [3].

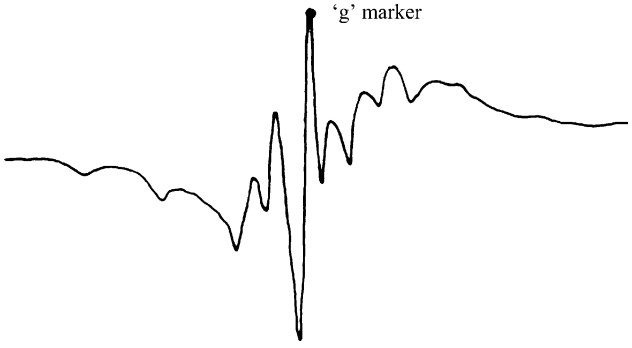

Fig. 4. EPR spectrum of [VO(ATABZ) SO_4 H_2O] at LNT.

In the electronic spectrum of oxovanadium(IV) complex, the two spin allowed transitions observed at 11,100 and 16,638 cm^{-1} were due to the $^2B_2 \rightarrow E$ and $^2B_2 \rightarrow {}^2B_1$, respectively as expected for a C_{4V} symmetry. The third band due to $^2B_2 \rightarrow {}^2A_1$ transition was masked by the strong charge transfer transition and hence was not observed [22,23]. A magnetic moment value of 1.72 BM was obtained as expected for an $S = 1/2$ system.

3.4. IR spectra

In order to ascertain the mode of bonding of ATABZ to the metal ions, the IR spectra of the free ligand was compared with those of its metal complexes. The diagnostic IR bands are given in Table 4.

The IR spectrum of ATABZ exhibits two sharp bands of medium intensity at 3469 and 3353 cm^{-1} which are assigned to the ν_{asym} and ν_{sym} stretching frequencies of the free NH_2 group, respectively [24]. A broad band at 3200 cm^{-1} is due to NH stretching frequency of the amide moiety. Three strong vibrations at 1629, 1537 and 1255 cm^{-1} are ascribed to the amide I (νC=O), amide II and amide III bands respectively [25]. The appearance of the νC=O band at a relatively lower wave number is due to the presence of strong intra molecular hydrogen bonding between free NH_2 and carbonyl oxygen, which is supported by single crystal X-ray study. A weak band at 1606 cm^{-1} is due to the νC=N of the azomethine group whereas the band at 1015 cm^{-1} is assigned to the νN–N [3].

The medium intensity band at 1355 cm^{-1} is ascribed to the ring stretching vibration of the νCSC of the thiophene moiety [26].

In the IR spectra of all the complexes, the bands due to the ν_{sym} and ν_{asym} modes of the free NH_2 group are shifted to higher frequency by 39–71 and 12–67 cm^{-1}, respectively indicating the breakdown of hydrogen bonding between NH_2 and >C=O group. The amide I(νC=O) undergoes a negative shift by 14–22 cm^{-1} in all the complexes followed by the upward shift of the amide II and III bands by 13–15 and 5–8 cm^{-1}, respectively. These changes indicate the involvement of carbonyl oxygen in coordination to the metal [25]. The azomethine frequency is shifted to lower wave number in all the complexes indicating ligation of azomethine nitrogen to metal which is further supported by an increase in the νN–N band by 13–22 cm^{-1} [22]. The νCSC vibration remains almost unperturbed in all the complexes indicating the non-participation of the sulphur atom in coordination [26].

3.5. NMR spectra

In order to study the hydrogen bonding interactions in the solution state, and to assign the respective protons and carbons, the 2D HETCORR NMR study of ATABZ was carried out. The ^1H NMR spectra of ATABZ and its cadmium(II) complex were recorded in dmso-d_6. The spectral assignments were made based on comparisons with NMR assignments of methyl anthranilate [27], 2-acetylthiophene [28] and 2D HETCORR

Table 4
IR spectral assignments of ATABZ and its transition metal complexes

Compound	$\nu(NH_2)$		ν(C=O)amide	ν(C=N)	ν(NH) amide	Amide II	Amide III	ν(N-N)	ν(CSC)
	ν_{asym}	ν_{sym}							
ATABZ	3469sh	3353sh	1629s	1606m	3200m	1537s	1255s	1015m	1355m
(Cd(ATABZ)Cl_2)	3505sh	3402sh	1612s	1587m	3258m	1550m	1260m	1028m	1357m
(Co(ATABZ)Cl_2)	3515 sh	3383sh	1606s	1592m	3274m	1552m	1255m	1037m	1356m
(Cu(ATABZ)Cl_2)	3478 sh	3365sh	1618s	1598m	3275m	1552m	1252m	1035m	1358m
(Ni(ATABZ)Cl_2))	3463 sh	3372sh	1615s	1597m	3273m	1553m	1252m	1034m	1355m
(Mn(ATABZ)Cl_2)	3480 sh	3375sh	1616s	1596m	3273m	1553m	1255m	1035m	1353m
(Zn(ATABZ)Cl_2)	3485 sh	3376sh	1615s	1593m	3277m	1550m	1263m	1030m	1354m
((VO(ATABZ)SO_4 H_2O)	3540sh	3420sh	1615s	1592m	3278m	1552m	1263m	1029m	1355m

sh, sharp; *s*, strong; *m*, medium.

NMR of ATABZ. The ^1H and ^{13}C NMR data for ATABZ and its cadmium(II) complex is given in Table 5. The numbering scheme for the assignments of carbons and protons is given in Scheme 1. and the 2D HETCORR of ATABZ is displayed in Fig. 5.

The NH proton resonates as a singlet in the downfield region (10.51 ppm). The resonance due to the methyl protons was observed as a singlet at 3.34 ppm while that of NH_2 also appeared as a singlet at 6.22 ppm. The aromatic protons of the phenyl ring are observed as doublets at 7.60 [H10] and 6.76 [H13] and as triplets at 7.20 [H12] and 6.58 ppm [H11]. The signals at 7.50, 7.10 and 7.54 ppm were observed as a doublet, triplet and doublet, respectively and are assigned to H2, H3 and H4 of the thiophene moiety

In the ^1H NMR spectrum of the cadmium(II) complex, the NH singlet undergoes an upfield shift to 9.56 ppm probably due to the breakdown of intra molecular hydrogen bonding between carbonyl oxygen and amide NH upon complexation. The H10, H4 and H2 signals are merged together and shifted upfield to give a multiplet at 7.42 ppm. A triplet at 7.15 ppm is due to the merger of the H12 and H3. The H13 and H11 signals undergo a slight up field shift of 0.06 and 0.09 ppm respectively whereas the methyl singlet remains almost unperturbed.

The ^{13}C NMR spectrum of ATABZ showed a signal at 166.21 ppm assigned to the carbonyl carbon (C8) whereas a peak at 3.34 ppm is due to the methyl carbon (C7). The signals due to the quaternary carbons C5, C6, C8, C9 and C14 were observed at 132.49, 150.07, 166.21, 115.0 and 143.94 ppm. In the ^{13}C NMR spectrum of the cadmium(II) complex the C8 and C6 signals are shifted downfield to 167.52 and 150.86 ppm indicating the involvement of carbonyl oxygen and azomethine nitrogen in ligation, respectively. All the other signals remain almost unperturbed.

3.6. Thermal studies

The thermograms of the representative nickel(II) and zinc(II) complexes have been recorded. The nickel(II) complex decomposes in two steps. In the first step, the weight loss of 18.1% (Calcd 18.2%) in the 230–350 °C temperature range is due to the loss of two coordinated chlorides. Further weight loss of 66.6% (Calcd 66.65%) between 360–580 °C is assigned to the loss of a ligand molecule. Finally the most stable oxide NiO is formed. The metal percentage of 15.0% is in agreement with the values obtained by metal determinations (Calcd 15.1%).

In the case of the zinc(II) complex a weight loss of 83.3% (Calcd 83.4%) in the 200–600 °C region is due to the loss of two coordinated chlorides and a ligand molecule. The plateau obtained on heating above 600 °C with a residual weight of 20.5% (Calcd 20.5%) accounts for the formation of stable ZnO and tallies with the metal analysis (16.5%).

3.7. Biological activity

The antibacterial and antifungal activities of the ATABZ and its transition metal (II) complexes were evaluated against the bacteria *Pseudomonas aeuregenosa* (PA) (Gram negative)

Table 5
^1H and ^{13}C NMR data of ATABZ and its cadmium(II) complex

Position	ATABZ		Cd(II) complex*	
	^{13}C	^1H	^{13}C	^1H
NH	–	10.51 (s)	–	9.56 (s)
C2	128.43	7.50 (d, $J=3.4$)[a]	128.44	–
C3	128.00	7.10 (t, $J=4.5$)[b]	128.02	–
C4	129.28	7.54 (d, $J=7.7$)[a]	129.52	7.42 (m)
C5	132.49	–	132.59	–
C6	150.07	–	150.86	–
C7	15.21	3.34(s)	15.20	3.31 (s)
C8	166.21	–	167.52	–
C9	115.0	–	115.0	–
C10	129.51	7.60 (d, $J=4.9$)[a]	129.27	–
C11	115.23	6.58 (t, $J=7.4$)	115.22	6.49 (t, $J=7.1$)
C12	132.49	7.20 (t, $J=7.5$)[b]	132.50	7.15 (t, $J=7.71$)
C13	116.91	6.76 (d, $J=8.2$)	116.69	6.7 (d, $J=8.1$)
C14	143.94	–	143.98	–
NH_2	–	6.22 (s)	–	6.20 (s)

m, multiplet; *d*, doublet; *t*, triplet; *s*, singlet. *The splitting pattern was obscured due to the poor solubility of the compound in DMSO.
[a] These protons appear as a multiplet in the complex.
[b] These protons appear as a triplet in the complex.

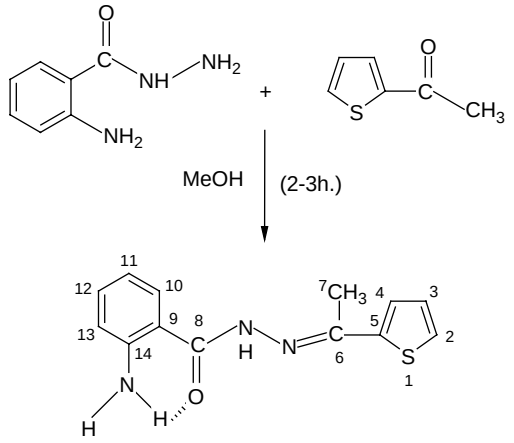

Scheme 1.

and *Bacillus cirroflagellosus* (BC) (Gram positive) and the fungi *Aspergillus niger* (AN) and *Penicillium notatum* (PN), by the cup-plate method [29] and are compiled in Table 6. The concentration of the compound used for testing was 1 mg/ml in DMSO. Grisofulvin and Norfloxacin were the standards used against fungi and bacteria respectively.

The ligand ATABZ was found to be less active against all the organisms. The complexes were found to be less active against the fungi PN and AN. In case of bacteria, all the complexes were found to be moderately active against the Gram negative bacteria PA and Gram negative BC except Mn(II) complex which was less active against PA. The enhanced activity of some complexes, compared to the ligand and metal salts (inactive) alone has been attributed to the synergistic effect [30]. According to Tweedy's chelation theory [31], on chelation, the polarity of metal ion decreases due to partial sharing of its positive charge with the ligand, which further leads to enhancement of lipophilicity of the complex. Increased lipophilicities allow for penetration of complexes into, and through the lipid membrane of micro organisms and inactivation of the enzyme active sites.

4. Conclusions

Based on the various studies, it is concluded that the ligand ATABZ reacts with the transition metal salts to give mononuclear four-coordinate complexes of 1:1 stoichiometry having the formula $[M(ATABZ).Cl_2]$ [Fig. 6] in the case of cobalt(II), manganese(II), copper(II), nickel(II), zinc(II) and

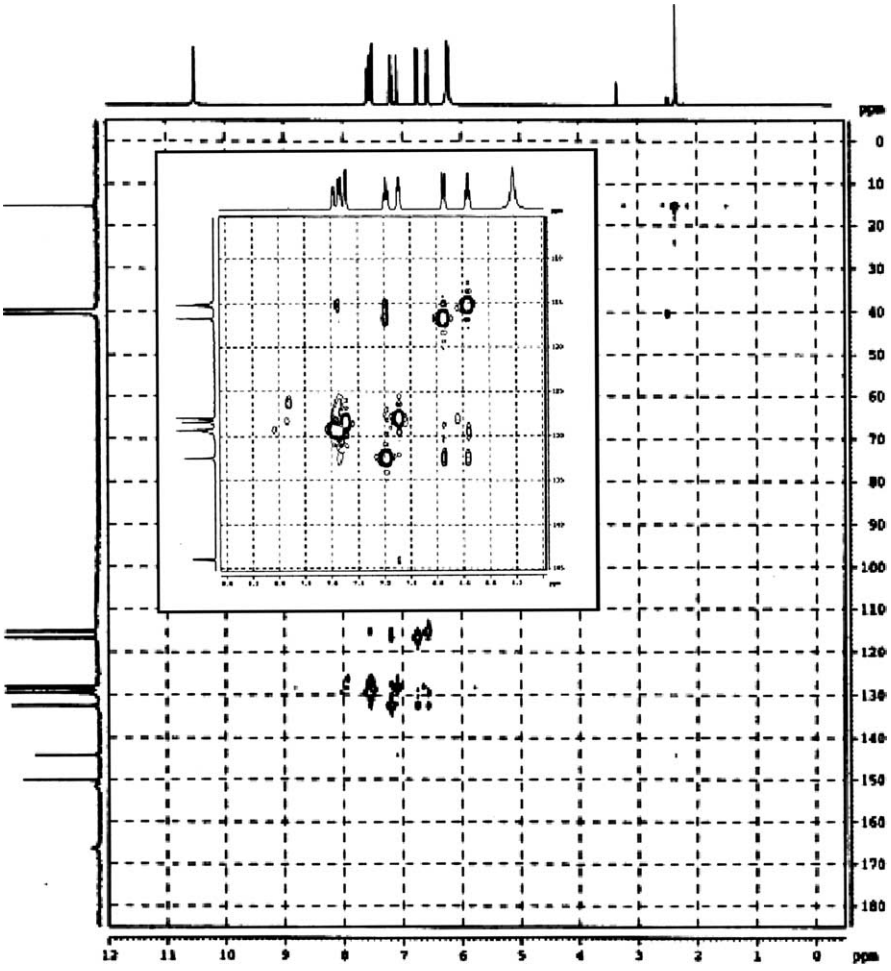

Fig. 5. 2D HETCORR NMR spectrum of ATABZ (Expanded form is shown in the box inset).

Table 6
Antibacterial and antifungal activity data of ATABZ and its pransition metal complexes

Compound	Antifungal		Antibacterial	
	PN	AN	PA	BC
ATABZ	+	+	+	+
(VO(ATABZ)SO_4 H_2O)	+	+	++	++
(Mn(ATABZ)) Cl_2	+	+	+	++
(Co(ATABZ)) Cl_2	+	+	++	++
(Cu(ATABZ)) Cl_2	+	+	++	++
(Ni(ATABZ)) Cl_2	+	+	++	++
(Zn(ATABZ)) Cl_2	+	+	++	++
(Cd(ATABZ)) Cl_2	+	+	++	++
Grisofulvin	+++	+++	–	–
Norfloxacin	–	–	+++	+++
Control	–	–	–	–

Key to interpretation: PN, *Penicillium notatum*; AN, *Aspergillus niger*; PA, *Pseudomonas aeuregenosa*; BC, *Bacillus cirroflagellosus*; (−)No zone, inactive; 1–5 mm (+), Less active; 6-10 mm (++), moderately active; 11–15 mm (+++), highly active.

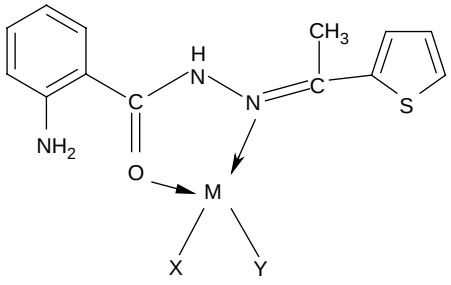

Fig. 6. Tentative structure of [M(ATABZ).X.Y] complexes X = Y = Cl in case of Co(II), Mn(II), Cu(II), Ni(II), Zn(II) and Cd(II). X = H_2O, Y = SO_4 in case of VO(IV).

cadmium(II) and a five-coordinate complex [VO(ATABZ)·H_2O·SO_4] in the case of oxovanadium(IV). IR and NMR spectral studies indicate that the ligand behaves in bidentate fashion coordinating through carbonyl oxygen and azomethine nitrogen with the NH_2 and thiophene sulphur remaining unligated. Antimicrobial studies indicate the complexes to be moderately active against the bacteria whereas they were less active against the fungi.

Acknowledgements

Thanks are due to S.I.F, I.I.Sc., Bangalore, I. I. T., Bombay and U.S.I.C., Karnatak University, Dharwad for recording NMR, EPR and UV-VIS spectra, respectively. Authors are thankful to Prof S. B. Padhye, University of Pune, India for magnetic measurement facilities.

References

[1] Y.P. Kitaev, B.I. Buzykin, T.V. Troepolskaya, Russ. Chem. Rev. 39 (6) (1970) 441.
[2] M. Bakir, I. Hassan, T. Johnson, O. Brown, O. Green, C. Gyles, M.D. Coley, J. Mol. Struct. 688 (2004) 213.
[3] A.E. Dissouky, O.A. Fulij, S.S. Kandil, J. Coord. Chem. 57 (7) (2004).
[4] N. Nawar, N.M. Hosny, Chem. Pharm. Bull. 47 (7) (1999) 944.
[5] M. Vasu, B.H. Doreswamy, K.A. Nirmala, J. Saravanan, S. Mohan, M.A. Sridhar, J.S. Prasad, Anal. Sci. 20 (2004) 21.
[6] D.J. Rance, in: L.A. Damani (Ed.), Sulfur-Containing Drugs and Related Organic Compounds, vol. 1, Ellis Horwood, Chichester, 1989 (part B, Chapter 9).
[7] Shailendra.N. Bharti, F. Naqvi, A. Azam, Bioorg. Med. Chem. Lett. 13 (4) (2003) 689.
[8] A. Maiti, S. Ghosh, J. Inorg. Biochem. 36 (1989) 131.
[9] R. Dinda, P. Sengupta, S. Ghosh, H. Mayer-Figge, W.S. Sheldrick, J. Chem. Soc., Dalton Trans. (2002) 4434.
[10] S. Ianelli, P. Mazza, M. Orcesi, C. Pelizzi, G. Pelizzi, F. Zani, J. Inorg. Biochem. 60 (1995) 89.
[11] M.F. Simeonov, F. Fulop, R. Sillanpaa, K. Pihlaja, J. Org. Chem. 62 (1997) 5089.
[12] K.K. Narang, J.P. Pandey, V.P. Singh, Polyhedron 13 (1994) 529.
[13] G.M. Sheldrick, SHELXL 97 Program for the Solution of Crystal Structures, University of Gottingën, Germany, 1997.
[14] W.J. Geary, Coord. Chem. Rev. 7 (1971) 81.
[15] C.K. Johnson, ORTEP REPORT ORNL 3794, Oak Ridge National Laboratory, Tennessee.
[16] S. Ianelli, P. Mazza, M. Orcesi, C. Pelizzi, G. Pelizzi, F. Zani, J. Inorg. Biochem. 60 (1995) 89.
[17] J.P. Conde, M.R.J. Elsegood, K.S. Ryder, Acta Crystallogr., Sect. C 60 (2004) 166.
[18] Y.M. Chumakov, B.Y. Antosyak, M.D. Mazus, V.I. Tsapkov, N.M. Samus, J. Struct. Chem. 41 (5) (2000) 905.
[19] D. Kivelson, R. Nieman, J. Chem. Phys. 35 (1961) 149.
[20] B.J. Hathaway, D.E. Billing, Coord. Chem. Rev. 5 (1970) 143.
[21] D. Kivelson, S.K. Lee, J. Chem. Phys. 41 (1964) 1896.
[22] K.K. Nanda, S. Mohanta, S. Ghosh, M. Mukherjee, M. Helliwell, K. Nag, Inorg. Chem. 34 (1995) 2861.
[23] C. Ballhausen, H.B. Gray, Inorg. Chem. (1962) 111.
[24] O.P. Pandey, Polyhedron 6 (5) (1987) 1021.
[25] S.K. Sahni, S.P. Gupta, S.K. Sangal, V.B. Rana, J. Indian Chem. Soc. (1987) 200.
[26] A. El-Dissouky, A.K. Shehata, G. El-Mahdey, Polyhedron 16 (7) (1997) 1247.
[27] SDBS web: http://www.aist.go.jp/RIODB/SDBS (27-8-2004), SDBS No. 730 HSP-40-980.
[28] SDBS web:http://www.aist.go.jp/RIODB/SDBS (2-9-2005) SDBS No. 1647 HSP-04-075.
[29] F. Cavanagh, Analytical Microbiology, Academic Press, New York, 1963.
[30] S.S. Kukalenko, B.A. Borykin, S.I. Sheshtakova, A.M. Umelchenko, Russ. Chem. Rev. 54 (7) (1985).
[31] B.G. Tweedy, Phytopathology 55 (1964) 910.